

REFERENCES

1. Hara, T., Yokoi, M. and Kato, S., "Study on Thermal Plumes in Free Space by Means of Numerical Simulation Based on Standard $k-\epsilon$ Model", J. Archit. Plann. Environ. Eng., AIJ, No.530, Apr., 2000
2. Hara, T., Yokoi, M. and Kato, S., "Analysis of Thermal Plumes with Numerical Simulation Part5, Influence of Heat Conduction through Walls on Numerical Solution of Corner Plumes", Summaries of Technical Papers of Annual Meeting, Architectural Institute of Japan, pp. 145~146, Sept., 1999
3. Hara, T., Yokoi, M. and Kato, S., "Analysis of Thermal Plumes with Numerical Simulation and Experimental Results Part4, Influence of Mesh Division on Numerical Solution to Corner Plumes", Proceedings of Annual Meeting of JAFSE, pp.396~399, May, 1999
4. Yokoi, M., Hara, T. and Kato, S., "Analysis of Thermal Plumes with Numerical Simulation and Experimental Results Part3, Influence of Numerical Scheme, Compressible Model and Incompressible Model on Numerical Solution", Proceedings of Annual Meeting of JAFSE, pp.392~395, May, 1999
5. Cetegen, B.M., Zukoski, E.E. and Kubota, T., NBS-GCR-82-402, Entrainment and Flame Geometry of Fire Plumes, U.S. Department of Commerce, National Bureau of Standards, pp. 63,74~75, Aug., 1982
6. Klote, J. H., Milke, J. A., Design of Smoke Management Systems, American Society of Heating, Refrigerating and Air-Conditioning Engineers, Inc., pp.110~111, 1992
7. Takahashi, W., Sugawa, O. and Nara, M., "Properties of a Corner Fire", Proceedings of Annual Meeting, JAFSE, pp.84~87, May, 1994
8. Tanaka, H., Takahashi, W., Nara, M., Sugawa, O. and Segawa, R., "Flame Height Behavior in and beside a Corner", Summaries of Technical Papers of Annual Meeting, Architectural Institute of Japan, pp.1379~1380, Sept., 1994
9. Takahashi, W., Sugawa, O. and Tanaka, H., "Properties of Flame/Plume Behavior in and near a Corner", Summaries of Technical Papers of Annual Meeting, Architectural Institute of Japan, pp.45~46, Aug., 1995
10. Takahashi, W., Sugawa, O. and Ohtake, M., "Flame and Plume Behavior in and near a Corner of Wall", Proceedings of Annual Meeting, JAFSE, pp.306~307, May, 1997
11. Sugawa, O., Takahashi, W., Ohtake, M. and Satoh, H., "A Study on Fire Characteristics in a Tall and Narrow Atrium", International Symposium on Fire Science and Technology, 1997
12. Tobari, T., Sugawa, O., "Flame Behavior in and near Room Corner", Proceedings of Annual Meeting, JAFSE, pp.326~329, May, 1999
13. Yokoi, S., "Study on the Prevention of Fire-Spread Caused by Hot Upward Current", Report of the Building Research Institute, No.34, Nov., 1960
14. Murakami, S., Kato, S. and Suyama, Y., "Analysis of Finite Difference Schemes for Convective Terms such as Quick Scheme or Other Schemes, Study on Diagnostic System for Numerical Simulation of Turbulent Flow in Room (Part2)", J. Archit. Plann. Environ. Eng., AIJ, No.390, pp.1~12, Aug., 1988
15. Murakami, S., Kato, S. and Nagano, S., "Estimation of Error Caused by Coarseness of Finite-Differencing, Study on Diagnostic System for Simulation of Turbulent Flow in Room (Part1)", J. Archit. Plann. Environ. Eng., AIJ, No.385, pp.9~17, Mar., 1988

A Numerical Study of Smoke Movement in Atrium Fires with Ceiling Heat Flux

J.Y. JEONG, H.S. RYOU, S.C. KIM and C.I. KIM

Department of Mechanical Engineering, Chung-Ang University
221 Huksuk-Dong, Dongjak-Ku, Seoul 156-756, Korea

ABSTRACT

This paper describes the smoke filling process of a fire field model based on a self-developed SMEP(Smoke Movement Estimating Program) code to the simulation of fire induced flows in the two types of atrium space containing a ceiling heat flux. The SMEP using PISO algorithm solves conservation equations for mass, momentum, energy and species, together with those for the modified $k-\epsilon$ turbulence model with buoyancy term. Compressibility is assumed and the perfect gas law is used. Comparison of the calculated upper-layer average temperature and smoke layer interface height with the zone models has shown reasonable agreement. The zone models used are the CFAST developed at the Building and Fire Research Laboratory, NIST, U.S.A. and the NBTC one-room of FIRECALC developed at CSIRO, Australia. For atrium with ceiling glass the consideration of the ceiling heat flux by solar heat may be necessary in order to produce more realistic results. The smoke layer interface heights that are important in fire safety were not as sensitive as the smoke layer temperature to the nature of ceiling heat flux condition. This study highlights the utility of SMEP field modeling for the analysis of smoke movement and temperature in atrium fires.

KEY WORDS: Smoke filling process, heat flux, SMEP, Atrium, Field model, Zone model

INTRODUCTION

In recent years, the atrium building has become commonplace. Other large open spaces include enclosed shopping malls, arcades, sports arenas, exhibition halls and airplane hangers. The smoke generated from fires in these spaces may cause people to panic and interfere with evacuation. Not only does the smoke generated from modern synthetic materials lead to disorientation and death of the occupants, but also large quantities of smoke become an obstacle to fire extinction. Therefore fire safety is an important issue to be considered by architects and engineers when they design the fire protection systems such as sprinklers and smoke control systems etc. However, there are few design guides with strong scientific backgrounds suitable for use by the construction industry.

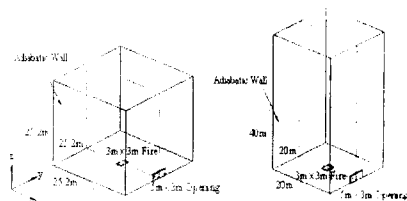
The ability of sprinklers to suppress fires in spaces with ceilings higher than 11 to 15m is limited[1,2]. Because the temperature of smoke decrease as it rises(due to entrainment of ambient air), smoke may not be hot enough to activate sprinklers mounted under the ceiling of

an atrium. Even if such sprinklers activate, the delay can allow fire growth to an extent beyond the suppression ability of ordinary sprinklers. Thus architects and engineers have to consider the smoke movement and temperature in atrium spaces. Many of the space characteristics of an atrium differ from traditional buildings. For example, if a fire occurs in the atrium, flame and smoke will spread vertically rather than horizontally to those parts of the building surrounding the atrium. The fire products are driven upwards within the interior of the atrium due to buoyancy force. It is difficult to control smoke movement in such a case with the conventional ventilation designs available [3]. Some studies have been done concerning prediction of smoke movement and temperature in atrium spaces [4-6]. Also, as the smoke movement is effected by a large number of inter-dependant processes including the stack effect and wind pressure, it is difficult and expensive to perform experimental studies with full-scale models. The alternative is to use computer simulation methods to determine the important physical parameters.

This study uses a self-developed SMEP field model [7] to the simulation of the smoke filling process in the two types of atrium spaces. The SMEP using PISO algorithm solves conservation equations for mass, momentum, energy and species, together with those for the modified k-epsilon turbulence model with buoyancy term. Compressibility is assumed and the perfect gas law is used. The SMEP are able to predict hot smoke temperature and smoke layer interface height which are most important in fire safety considerations for atrium fires and offer data on required safe egress time. For atrium with ceiling glass the consideration of the ceiling heat flux by solar heat may be necessary in order to produce more realistic results. Also, this research compares the results with the zone model and SMEP field model. The zone models used are the CFAST developed at the Building and Fire Research Laboratory, NIST, U.S.A. and the NBTC one-room of FIRECALC developed at CSIRO, Australia. It is hoped to offer engineers and architects essential data for smoke movement in an atrium fires.

PHYSICAL PROBLEM

In the simulation, two atrium buildings of same volume, $16,000\text{m}^3$, classified as type 1 and 2, are considered. Type 1 is of length 25.2m, width 25.2m and height 25.2m; and type 2 is of length 20m, width 20m and height 40m. The configurations and



(a) Type 1 atrium (b) Type 2 atrium
FIGURE 1: Geometry of the atrium halls

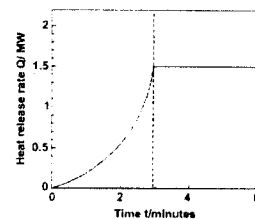


FIGURE 2: Heat release rate used for the fire simulation

dimensions of the two atrium spaces are shown in figure 1. In each case, there is a five meter wide by three meter high opening on the ground floor. A $3\text{m} \times 3\text{m}$ fire was located at the center of the floor. The heat release rate of the fire, $Q(\text{in MW})$, was increased as the square of time $t(\text{in s})$ and described by a fast mode of T^* fire in the simulation as:

$$Q = 47t^2 \quad (1)$$

The fire was then kept at 1.5MW after 178.6s as shown in figure 2. For atrium with the flow induced by this fire source is turbulent because the inertial force due to the density difference between the hot smoke and the ambient air is much greater than the viscous force. In this simulation, the modified k-epsilon turbulence model with buoyancy term is used. The intensity of solar radiation passing into the ceiling glass during winter relative to summer is high. By considering the transmission and angle of incidence into a building through ceiling glass at noon of the winter a constant ceiling heat flux of 620W/m^2 was used.

MATHEMATICAL MODEL

We consider a thermally expandable ideal gas driven by a prescribed heat source. The equations of motion governing the fluid flow are written in a form suitable for low Mach number applications. Sometimes, this form of the equations is referred to as "weakly compressible". The most important feature of these equations is that in the energy conservation equation the spatially and temporally varying pressure is replaced by an average pressure which depends only on time.

The flow is described by the three-dimensional, Favre-averaged equations of transport for mass, momentum, gas species concentration and internal energy. Turbulence is modeled using the modified k-epsilon equation model, with the turbulent viscosity given by $\mu_t = c_\mu \rho k^2 / \epsilon$. Terms (G_B in Table 1) were included in the modified k and ϵ equations to allow for the production of turbulence due to buoyancy and the effect of thermal stratification of the turbulence dissipation rate. The eight conservation equations were cast into the following form:

$$\frac{\partial}{\partial t}(\rho\phi) + \frac{\partial}{\partial x_j}(\rho u_j \phi) = \frac{\partial}{\partial x_j}(\Gamma_\phi \frac{\partial \phi}{\partial x_j}) + S_\phi \quad (2)$$

The variables, together with the exchange coefficients and source terms, are given in Table 1.

As there is no analytical solution for the set of equation, they are discretized into finite difference forms by the integral of the governing equation over the control volume and are solved numerically at those nodal points. Equation (2) can be discretized as the following form [8].

$$a_{nb} \phi_{nb} = \sum_{nb} a_{nb} \phi_{nb} + b \quad (3)$$

$$\text{where, } a_p = \sum_{nb} a_{nb} + \rho \frac{\Delta V}{\Delta t} + S_p, \quad b = S_c + \rho \phi_p \frac{\Delta V}{\Delta t} \quad (4)$$

where the subscript *nb* denotes a neighbor node, and the summation is to be taken over all the neighbors. Numerical methods are then employed for solving the linked set for velocity and pressure equations. The mathematical derivation and the experimental verification of the results are reported elsewhere [9,10] and will not be repeated here. As a summary, the assumptions made in SMEP are as follows.

TABLE 1. The Flux and Source Terms for the Conservation Equations

Φ	Γ_Φ	S_Φ
1	0	0
<i>u</i>	μ_{eff}	$-\frac{\partial p}{\partial x} + \frac{\partial}{\partial x}(\mu_{eff} \frac{\partial u}{\partial x}) + \frac{\partial}{\partial y}(\mu_{eff} \frac{\partial v}{\partial x}) + \frac{\partial}{\partial x}[\mu_{eff} \frac{\partial u}{\partial x} - \frac{2}{3}(\rho k + \mu_{eff} \nabla \cdot \vec{u})]$
<i>v</i>	μ_{eff}	$-\frac{\partial p}{\partial y} + \frac{\partial}{\partial x}(\mu_{eff} \frac{\partial u}{\partial y}) + \frac{\partial}{\partial y}(\mu_{eff} \frac{\partial v}{\partial y}) + \frac{\partial}{\partial y}[\mu_{eff} \frac{\partial v}{\partial y} - \frac{2}{3}(\rho k + \mu_{eff} \nabla \cdot \vec{u})]$
<i>w</i>	μ_{eff}	$-\frac{\partial p}{\partial z} + \frac{\partial}{\partial x}(\mu_{eff} \frac{\partial u}{\partial z}) + \frac{\partial}{\partial y}(\mu_{eff} \frac{\partial v}{\partial z}) + \frac{\partial}{\partial z}[\mu_{eff} \frac{\partial w}{\partial z} - \frac{2}{3}(\rho k + \mu_{eff} \nabla \cdot \vec{u})] + g(\rho_r - \rho)$
<i>e</i>	$\frac{\mu_{eff}}{\sigma_e}$	$-\rho \nabla \cdot \vec{u}$
<i>k</i>	$\frac{\mu_{eff}}{\sigma_k}$	$G_k + G_H - \rho \epsilon$
ϵ	$\frac{\mu_{eff}}{\sigma_\epsilon}$	$\frac{\epsilon}{k} [C_1(G_k + C_4 G_H) - C_2 \rho \epsilon] + C_3 \rho \epsilon \nabla \cdot \vec{u}$
<i>f</i>	$\frac{\mu_{eff}}{\sigma_f}$	0
$G_k = \mu_{eff} (\frac{\partial u_x}{\partial x_j} + \frac{\partial u_j}{\partial x_x}) \frac{\partial u_x}{\partial x_j}, \quad G_H = \frac{\mu_{eff}}{\sigma_f} g \frac{1}{\rho} \frac{\partial \rho}{\partial z}, \quad \mu_{eff} = \mu + \mu_t$		
$\sigma_k = 1.0, \sigma_\epsilon = 1.22, \sigma_e = 0.64, \sigma_f = 1.0, \sigma_r = 0.7, C_\mu = 0.09, C_1 = 1.44, C_2 = 1.92, C_3 = -0.343,$ $C_4 = 1.44 \text{ for } G_H > 0 \text{ and is zero otherwise.}$		

The modified *k*- ϵ turbulence model containing buoyancy and compressible effect is used. The conservation equations are solved by a finite volume method. The difference scheme for discretizing the convection term into linear form is the hybrid scheme. The difference scheme for discretizing the time term is the Euler implicit scheme. The algorithm PISO is used for solving the velocity-pressure linked equations. The computations were carried out on a Pentium II 300 personal computer.

The fire environment due to the same fire, of heat release rate given by equation (1), in the two atria was simulated using the field model. The two atrium halls were divided into $31 \times 23 \times 24$ and $31 \times 21 \times 27$ computing cells along the x, y and z (vertical direction) directions of a Cartesian co-ordinate system for the type1 and 2 spaces, respectively. Within each time step, convergence was assumed if either the maximum number of iterations(100) was reached or the mass source residual fell to 1×10^{-3} . The time step used was 0.25s and simulation was performed up to five minutes as this was considered sufficient time for people to evacuate the atrium safely. With regard to computing time, the SMEP using PISO algorithm was executed on a Pentium II 300 PC and the computing time required was less than five hours.

From the predicted air flow pattern and temperature fields, the smoke layer interface height is obtained by inspecting the positions where there are 1 percent of smoke concentration. The hot layer temperature is then taken to be the average value over all at the control cells in the smoke layer with each cell having a volume $\Delta \tau_i$ and temperature T_i [6]:

$$T_{av} = \frac{\sum_{\text{cells in the smoke layer}} T_i \Delta \tau_i}{\sum_{\text{cells in the smoke layer}} \Delta \tau_i} \quad (5)$$

PLUME MODEL AND INLET CONDITION

The flame height depends on the fire geometry, the ambient conditions, the heat of combustion and the stoichiometric ratio. A relationship [11] for flame height that can be used for many fuels is

$$Z_{fl} = 0.235 \dot{Q}^{2/5} - 1.02 D_f \quad (6)$$

where, Z_{fl} = mean flame height, m;

\dot{Q} = heat release rate of the fire, kW;

D_f = diameter of fire, m.

The virtual origin of the plume, ΔZ_f (m), [12] is

$$\Delta Z_f = 1.02 D_f - 0.083 \dot{Q}^{2/5} \quad (7)$$

The virtual origin can be above the top of the fuel or below the fuel. The sign convention is: for the virtual origin above the top of the fuel ΔZ_f is negative, and for the virtual origin below the top of the fuel ΔZ_f is positive. The mass flow, \dot{m} (kg/s), of an axisymmetric plume at height Z_{fl} [13] is

$$\dot{m} = 0.071 \dot{Q}_c^{1/3} (Z_{fl} + \Delta Z_f)^{5/3} [1 + 0.026 \dot{Q}_c^{2/3} (Z_{fl} + \Delta Z_f)^{-5/3}] \quad (8)$$

where, \dot{Q}_c = convective heat release rate of fire, kW.

Because smoke was defined to include the air that is entrained with the products of combustion, all of the mass flow in the plume is defined as being smoke. It follows that equation (8) can be thought of as an equation for the production of smoke from a fire. The convective of the heat release rate, \dot{Q}_c , can be $\dot{Q}_c = \xi \dot{Q}$. Where ξ is the convective fraction of heat release. The convective fraction depends on the heat conduction through the fuel and the radiative heat transfer of the flames, but a value of 0.7 is often used for ξ . The average temperature of the plume can be obtained from a first law of thermodynamics analysis of the plume. For the steady plume the work is zero, and the changes in kinetic and potential energy are negligible. The first law leads to an equation for the plume temperature:

$$T_{zf} = T_{\infty} + \frac{\dot{Q}_c}{\dot{m}C_p} \quad (9)$$

where, T_{zf} = average plume temperature at elevation Z_{fl} , K;

T_{∞} = ambient temperature, K;

C_p = specific heat of plume gases, kJ/kgK.

Fire plumes consist primarily of air mixed with the products of combustion, and the specific heat of plume gases is generally taken to be the same as air. The density of air and plume gases is calculated from the perfect gas law. The absolute pressure is taken to be standard atmospheric pressure of 101,325 Pa, and the gas constant is taken to be that of air which is 287 J/kgK.

Expression for the vertical upward speed v at height Z_{fl} above a fire for thermal plumes in free spaces [13] is used:

$$v = 3.4 \left(\frac{g \dot{Q}_c}{C_p \rho_{\infty} T_{\infty}} \right)^{1/3} (Z_{fl} + \Delta Z_f)^{-1/3} \quad (10)$$

where, v = vertical upward speed of plume at height Z_{fl} , m/s;

g = acceleration due to gravity;

ρ_{∞} = density of ambient gas.

The inlet boundary conditions of fire source can be specified using the velocity v and temperature T_{zf} obtained from the above equations.

BOUNDARY AND INITIAL CONDITION

The initial temperature and pressure were assumed to be 293 K and 101,325 Pa. Adiabatic wall boundary was assumed on the all of the side walls except the opening door and ceiling

wall with heat flux by solar heat. The Neumann condition is applied at the door opening. In the present calculation, the wall functions are used to bridge the near wall region as follows:

$$\tau_w = \frac{\rho \kappa^{1/4} k_p^{1/2} \mu U_p}{\ln(E y_p^+)} \quad (11)$$

$$\text{where, } y_p^+ = \frac{\rho C_{\mu}^{1/4} k_p^{1/2} y_p}{\mu}$$

$\kappa = 0.42$ which is known as von Karmann constant. The subscript p refers to the first nodal point adjacent to the wall.

NUMERICAL RESULTS AND DISCUSSIONS

In the present study, the smoke filling process for the two types of atrium spaces were simulated using the two types of deterministic fire model: zone models and field model. The zone models used are the CFAST model developed at the NIST, USA and the NBTC 1-room model of FIRECALC developed at CSIRO, Australia. The field model is a self-developed SMEP field model based on computational fluid dynamics theories. Also, this paper describes the smoke movement and temperature distribution of SMEP code to the simulation of fire induced flows in the two types of atrium space containing a ceiling heat flux because the consideration of the ceiling heat flux by solar heat in atrium with ceiling glass is necessary in order to produce more realistic results.

The smoke layer interface heights and average temperatures of the simulated type 1 and type 2 atrium are shown in figure 3 to figure 6. For without ceiling heat flux, the results predicted by the two approaches are very similar. Thus, the SMEP field model is suitable for studying the smoke filling process in a large atrium space. In the type 1 atrium (figure 3) and the type 2 atrium (figure 5), the smoke layer interface heights predicted by the zone models and the

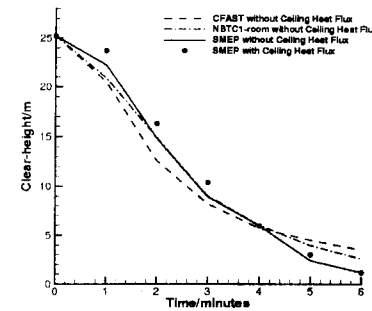


FIGURE 3: Smoke layer interface height in the type 1 atrium

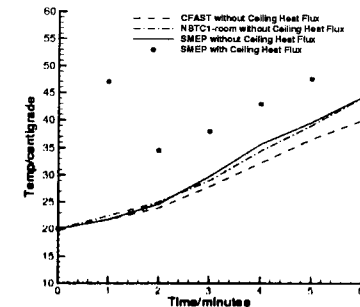


FIGURE 4: Smoke layer average temperature in the type 1 atrium

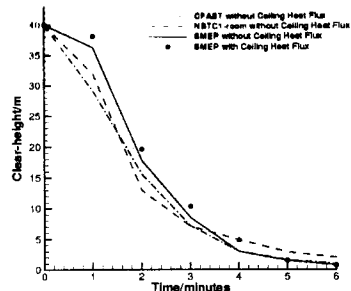


FIGURE 5: Smoke layer interface height in the type 2 atrium

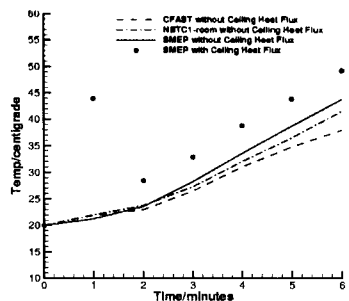


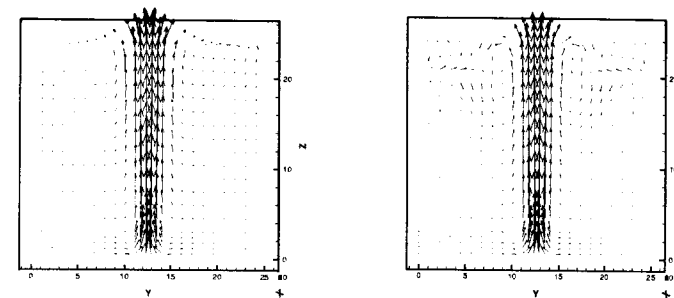
FIGURE 6: Smoke layer average temperature in the type 2 atrium

SMEP without ceiling heat flux and with ceiling heat flux have very similar trends. On the other hand, the smoke layer average temperatures predicted by the zone models and the SMEP without ceiling heat flux and with ceiling heat flux in figure 4 and figure 6 deviated quite a lot. For example, a difference of about 24°C in the early stage of a fire was found between the temperature predicted by the SMEP without ceiling heat flux and with ceiling heat flux. However, the results of the smoke average temperature after 1 minute increase linearly in proportion to a difference of about 8°C and 5°C, respectively. The results show that the smoke layer interface heights that are important in fire safety were not as sensitive as the smoke layer temperature to the nature of ceiling heat flux condition.

Figure 7 and figure 8 show velocity vectors at 60s and 180s in the type 1 atrium after starting the fire. Like all the other cases of fire simulation, air was entrained from bottom of the plume as shown in these figures. Also, fig. 7 and fig. 8 show re-circulation regions in the surroundings of smoke plume and complex phenomena for the SMEP with ceiling heat flux. These phenomena seem to come from the velocity induced by the temperature difference between hot ceiling and surrounding gas. The ceiling heat flux condition shows relatively small re-circulation region in the surroundings of smoke plume. This seems to come from the accumulation of smoke induced the reduction of buoyancy force by ceiling heat flux.

Figure 9 and figure 10 are the smoke temperature and the smoke concentration contours at 60s. Because of the elevated temperature, buoyancy forces drive gases upwards from the fire area towards the ceiling. In this way a plume is formed above the fire and relatively quiescent and cool gases at its periphery are laterally entrained and mixed with the plume gases. As a result of this entrainment the total mass flow in the plume continuously increases.

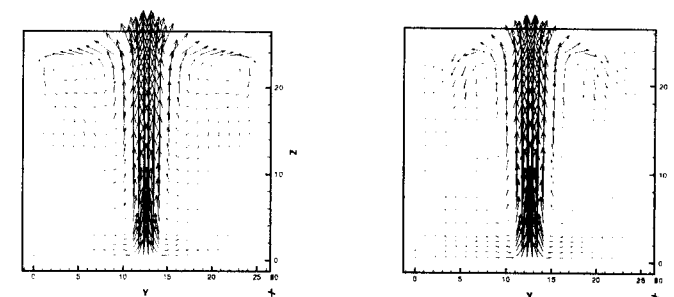
Figure 11 and figure 12 show smoke temperature contours at 180s. As depicted in fig. 9 to fig. 12, when the hot plume gases impinge on the ceiling, they spread across it forming a relatively thin radial jet and move outward under the ceiling surface. The hot gases transfer energy by convection and are retarded by frictional forces from the ceiling surface above, and by turbulent momentum transfer to the entrained air from below. As a result of all this flow and heat transfer, the ceiling jet continuously decreases in temperature, smoke concentration and velocity; and increase in thickness



(a) Without Ceiling Heat Flux

(b) With Ceiling Heat Flux

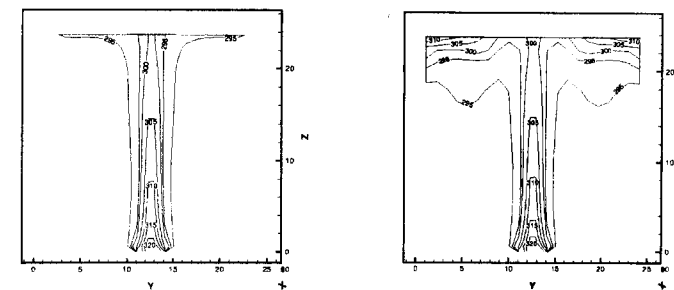
FIGURE 7: Velocity vectors for type 1 atrium at 60s



(a) Without Ceiling Heat Flux

(b) With Ceiling Heat Flux

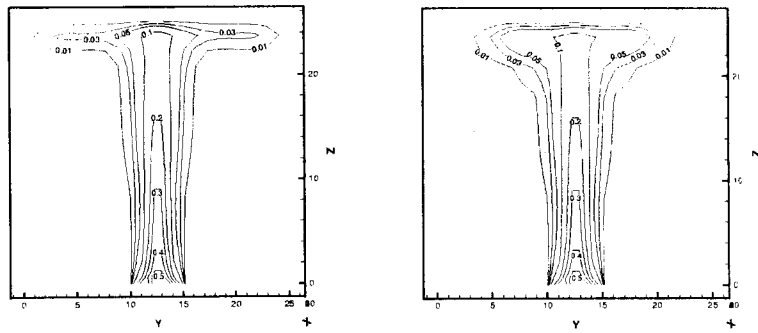
FIGURE 8: Velocity vectors for type 1 atrium at 180s



(a) Without Ceiling Heat Flux

(b) With Ceiling Heat Flux

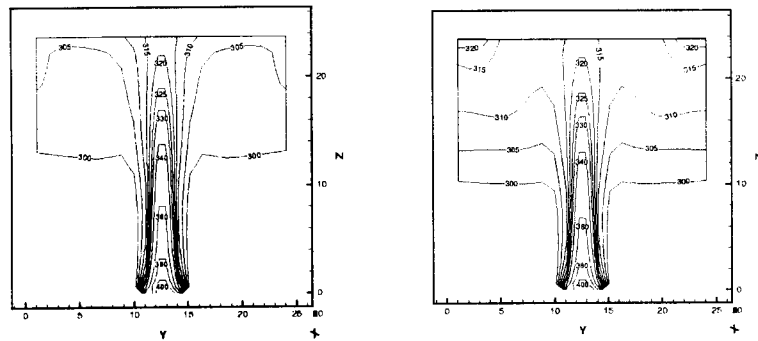
FIGURE 9: Temperature contours for type 1 atrium at 60s(All in K)



(a) Without Ceiling Heat Flux

(b) With Ceiling Heat Flux

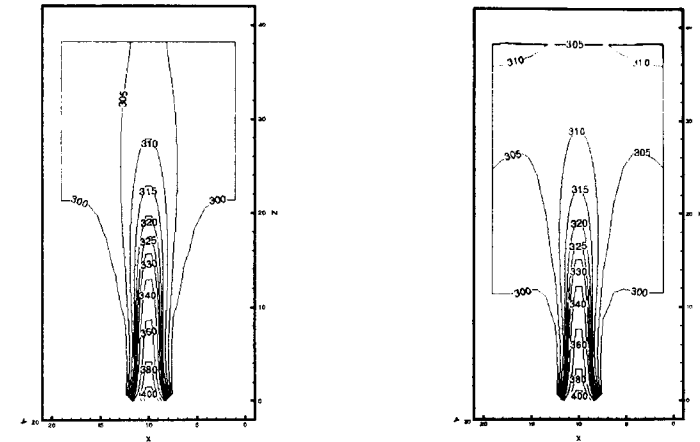
FIGURE 10: Gas concentration contours for type 1 atrium at 60s(All in $\times 100\%$)



(a) Without Ceiling Heat Flux

(b) With Ceiling Heat Flux

FIGURE 11: Temperature contours for type 1 atrium at 180s(All in K)



(a) Without Ceiling Heat Flux

(b) With Ceiling Heat Flux

FIGURE 12: Temperature contours for type 2 atrium at 180s(All in K)

with increasing radius. Because of the wall confining effect, the hot gases moved along the edge between the ceiling and the wall. The SMEP with ceiling heat flux has a high smoke temperature in near ceiling and forms a relatively thick radial jet. Also, because a low density induced by a high temperature near the ceiling decreases the buoyancy force and a low buoyancy and frictional force interfere with formation of downward wall jet the accumulation phenomenon of higher temperature than the surrounding temperature appears in the corner between the ceiling and the side wall. This phenomenon causes a high smoke temperature near the ceiling. However, this ceiling heat flux condition has no effect on the smoke movement such as the smoke layer interface height as shown in figure 3 and figure 4.

Figure 13 and figure 14 show the smoke average temperature below ceiling surface. For the early of the smoke formation near the ceiling after the start of a fire, a difference of a lot was found between the temperature predicted by the SMEP without ceiling heat flux and with ceiling heat flux but after about 3 minutes of the steady fire with constant heat release rate, 1.5MW, the temperature near the ceiling increases linearly in proportion to time.

CONCLUSIONS

The results for the smoke layer temperatures and the smoke layer interface heights, predicted by CFAST, NBTC 1-room's zone model and SMEP field model are very similar. Thus, the SMEP model is proposed to substitute the zone model for predicting the smoke layer temperatures and the smoke layer interface heights because zone models assume that a stable and homogeneous smoke layer is formed, even in a large atrium spaces.

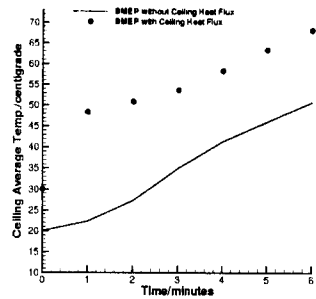


FIGURE 13: Smoke average temperature in the near ceiling for type 1 atrium

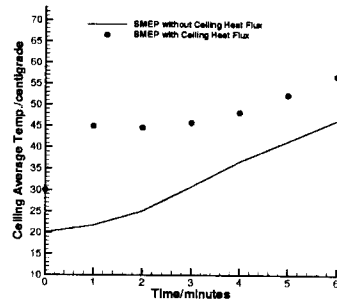


FIGURE 14: Smoke average temperature in the near ceiling for type 2 atrium

For no consideration of ceiling heat flux, a large re-circulation regions along the wall between the ceiling and the side are caused by the effect of relatively thin ceiling jet and downward wall jet. On the other hand, the SMEP with ceiling heat flux has a high smoke temperature in near ceiling and forms a relatively thick radial jet. Because a low density induced by a high temperature near the ceiling decreases the buoyancy force and this low buoyancy force and frictional force interfere with formation of downward wall jet the accumulation phenomenon of higher temperature than the surrounding temperature appears in the corner between the ceiling and the side wall. Also, this ceiling heat flux condition shows relatively small re-circulation region in the surroundings of smoke plume. These phenomena cause a high smoke temperature near the ceiling. However, this ceiling heat flux condition by solar heat has no effect on the smoke movement such as the smoke layer interface heights that are important in fire safety.

The smoke layer interface height is about 3m and 2m respectively at 5 minutes, regardless of ceiling heat flux, for the two types of atrium after starting the fire. Therefore, the required safe egress time in the two types of atrium is about 5 minutes. In conclusion, the smoke layer interface heights that are important in evacuation activity except the early of a fire were not as sensitive as the smoke layer temperature to the nature of ceiling heat flux condition. Thus, a fire sensor in a large atrium space has to consider these phenomena. Furthermore, additional quantitative validation of the model with experimental data must be performed. Work along all these lines is currently under way.

REFERENCES

1. Degenkolb, J.G., "Fire safety for Atrium Type Buildings", *Building Standards*, Vol. 44, No.2, pp. 16-18, 1975.
2. Degenkolb, J.G., "Atriums", *Building Standards*, Vol. 52, No. 1, pp. 7-14, 1983.

3. Kim, W.J., Yang, S.H. and Choi, K.R., "The Experimental Study of Fire Properties in Atrium Space of High-rise Buildings", *Journal of Korea Institute of Fire Science & Engineering*, Vol. 7, No. 2, pp. 13-23, 1993.
4. Notarianni, K.A. and Davis, W.D., "The Use of Computer Models to Predict Temperature and Smoke Movement in High Bay Spaces", National Institute of Standards and Technology, NISTIR 5304, 1993.
5. Chow, W.K. and Wong, W.K., "On the Simulation of Atrium Fire Environment Hong Kong using Zone Model", *Journal of Fire Science*, Vol. 11, pp. 3-51, 1993.
6. Chow, W.K., "A Comparison of the Use of Fire Zone and Field Models for Simulating Atrium Smoke-filling Process", *Fire Safety Journal*, Vol. 25, pp. 337-353, 1995.
7. Jeong, J.Y., Ryou, H.S. and Kim, S.C., "A Numerical Study of Smoke Movement for the Three Types of Atrium Fires using PISO Algorithm", *Journal of Korea Institute of Fire Science & Engineering*, Vol. 13, No. 1, pp. 21-30, 1999.
8. Patankar, S. V., *Numerical Heat Transfer and Fluid Flow*, pp. 25-40, McGraw Hill-Washington, D. C., 1980.
9. Peric, M., "A Finite Volume Method for the Prediction of Three Dimensional Fluid Flow in Complex Ducts", Ph.D., Imperial College, 1985.
10. Issa, R.I., "Solution of the Implicit Discretised Fluid Flow Equations by Operator-Splitting", *Journal of Computational Physics*, Vol. 62, NO. 1, pp. 40-65, 1985.
11. Heskestad, G., "Fire Plumes", SFPE Handbook of Fire Protection Engineering, Society of Fire Protection Engineers, Boston, MA, 1988.
12. Heskestad, G., "Virtual Origins of Fire Plumes", *Fire Safety Journal*, Vol. 5, No. 2, pp. 109-114, 1983.
13. Heskestad, G., "Engineering Relations for Fire Plumes", *Fire Safety Journal*, Vol. 7, No. 1, pp. 25-32, 1984.